SINR Analysis for V-BLAST with Ordered MMSE-SIC Detection

Ronald Böhnke and Karl-Dirk Kammeyer
Department of Communications Engineering
University of Bremen
Otto-Hahn-Allee NW1
28359 Bremen, Germany
{boehnke, kammeyer}@ant.uni-bremen.de

ABSTRACT

A new way to determine the exact layer-wise SINR distribution for V-BLAST with successive interference cancellation at the receiver is presented. In contrast to previous publications, we do not restrict to zero-forcing, but also consider minimum mean square error interference suppression. It is shown analytically that an optimized detection order has an even larger impact in this case. Numerical examples provide deeper insights into the underlying effects.

Categories and Subject Descriptors: G.3 [Probability and Statistics]: Distribution Functions

General Terms: Theory.

Keywords: V-BLAST, SINR Distribution, Zero-Forcing, MMSE, Ordered Successive Interference Cancellation.

1. INTRODUCTION

It is well known that very high spectral efficiencies can be achieved by using multiple antennas at the transmitter and the receiver [1]. One candidate for future mobile communication systems is the V-BLAST architecture [2], where independent data streams are transmitted from different antennas. A detailed performance analysis for simple linear as well as optimal maximum-likelihood receivers can be found in [3]. However, things become more complicated for the ordered successive interference cancellation (SIC) proposed in [2]. In [4], it was shown that without ordering the diversity order of the k-th layer is given by $N_R - N_T + k$, where N_T and N_R denote the number of transmit and receive antennas. The importance of an optimized detection order for the information outage probability was highlighted in [5], where a uniform power and rate allocation among a subset of transmit antennas was conjectured to be optimal. However, the required distribution of the layer-wise signal to noise ratio (SNR) with optimal ordering was only approximated by Monte-Carlo simulations. The exact expression for the case of two transmit antennas was determined in [6] using the distribution of the angle between two complex Gaussian vectors, which was also used to derive loose bounds for $N_T > 2$ in [7]. An alternative approach based on the inverted complex Wishart distribution was recently presented in [8].

The above mentioned publications assume perfect suppression of the remaining interference by a zero-forcing (ZF) filter. In this paper, we describe another and somewhat more direct method to calculate the SNR distribution of ordered ZF-SIC, and extend it afterwards to analyze also the signal to interference and noise ratio (SINR) if a minimum mean square error (MMSE) filter is applied instead. Expect for the simple case of unsorted ZF-SIC we will restrict to only two transmit antennas; although our basic approach may possibly be generalized, the resulting expressions become quite involved. Several illustrations help to gain intuition into the fundamental effects of optimizing the detection order and MMSE filtering.

IWCMC'06, July 3–6, 2006, Vancouver, British Columbia, Canada.

2. PRELIMINARIES AND NOTATION

Throughout this paper, vectors (matrices) are represented by bold lower (upper) case letters. $\mathbf{I}_n$ is an identity matrix of size $n \times n$, $\mathrm{E}\{\cdot\}$ the expectation operator, and $(\cdot)^T$ and $(\cdot)^H$ denote transpose and Hermitian transpose, respectively. We will frequently use the regularized incomplete gamma functions [9]

$$\tilde{\Gamma}(n,x) = \frac{\Gamma(n,x)}{\Gamma(n)} = \int_x^\infty \frac{t^{n-1}e^{-t}}{\Gamma(n)}\,dt = e^{-x}\sum_{m=0}^{n-1}\frac{x^m}{m!} \quad (1)$$

$$\tilde{\gamma}(n,x) = \frac{\gamma(n,x)}{\Gamma(n)} = \int_0^x \frac{t^{n-1}e^{-t}}{\Gamma(n)}\,dt = 1 - \tilde{\Gamma}(n,x) \quad (2)$$

for integer argument $n \geq 1$, and the integrals

$$\int_0^a \frac{t^{n-1}e^{-t}}{\Gamma(n)} \int_{b-ct}^\infty e^{-u}\,du\,dt = \begin{cases} \frac{e^{-b}\tilde{\gamma}(n,[1-c]a)}{[1-c]^n} & , c \neq 1 \\ \frac{a^n e^{-b}}{n!} & , c = 1 \end{cases} \quad (3)$$

as well as (for $b \neq 0$ and $b \neq c$)

$$\int_0^a e^{bt}\tilde{\gamma}(n,ct)\,dt = \frac{e^{ab}\tilde{\gamma}(n,ac)}{b} - \frac{c^n\tilde{\gamma}(n,[c-b]a)}{[c-b]^n b} \quad (4)$$

will be required. Finally, the abbreviations cdf and pdf stand for cumulative distribution function and probability density function.

3. SYSTEM MODEL

Consider the equivalent baseband model of a single-user multiple antenna system with N_T transmit and $N_R \geq N_T$ receive antennas. The channels are uncorrelated and flat Rayleigh fading. Hence, the $N_R \times N_T$ channel matrix $\mathbf{H}$ consists of independent circularly symmetric complex Gaussian entries with zero mean and unit variance. The receive vector is given by

$$\mathbf{y} = \mathbf{H}\mathbf{x} + \mathbf{n} \,, \tag{5}$$

where the vector $\mathbf{x} = [x_1, \dots, x_{N_T}]^T$ with covariance matrix $\mathrm{E}\left\{\mathbf{x}\mathbf{x}^H\right\} = \mathbf{I}_{N_T}$ contains independent transmit symbols, and $\mathbf{n}$ represents circularly symmetric and white complex Gaussian noise with variance σ_n^2. Perfect channel state information is assumed at the receiver.

4. ZF-SIC WITHOUT ORDERING

For each layer (i.e., the data stream of one specific transmit antenna), the following two steps are performed:

- The interference caused by already detected layers is subtracted from the receive signal.
- The interference of the remaining layers is suppressed by a linear filter.

The required filter matrices follow from the QL decomposition of the channel matrix $\mathbf{H} = \mathbf{QL}$, where the $N_R \times N_T$ matrix $\mathbf{Q}$ has orthogonal columns with unit norm and $\mathbf{L}$ is lower triangular with real-valued and nonnegative diagonal elements [10]. Multiplying $\mathbf{y}$ with $\mathbf{Q}^H$ results in

$$\mathbf{z} = \mathbf{Q}^H\mathbf{y} = \mathbf{L}\mathbf{x} + \tilde{\mathbf{n}} \,. \tag{6}$$

The noise at the filter output $\tilde{\mathbf{n}} = \mathbf{Q}^H\mathbf{n}$ is still white with variance σ_n^2. For $k = 1, \dots, N_T$, the estimate $\hat{x}_k$ of x_k can be obtained by quantizing

$$\tilde{x}_k = \frac{1}{l_{kk}}\left(z_k - \sum_{m=1}^{k-1} l_{km}\cdot\hat{x}_m\right) \tag{7}$$

$$= x_k + \sum_{m=1}^{k-1}\frac{l_{km}}{l_{kk}}(x_m - \hat{x}_m) + \frac{\tilde{n}_k}{l_{kk}} \tag{8}$$

to the discrete symbol alphabet. Assuming correct decisions in all previous detection steps (i.e., $\hat{x}_m = x_m$), the SNR of the k-th layer is given by

$$\mathrm{SNR}_k = \frac{l_{kk}^2}{\sigma_n^2} \,, \tag{9}$$

which is identical to the SINR, because the ZF filter completely removes all interference.

4.1 SNR Distribution

The QL decomposition may be interpreted as a special change of the coordinate system in which the matrix $\mathbf{H}$ is represented, with the columns of $\mathbf{Q}$ being the orthogonal base vectors. From the rotational invariance of the multivariate Gaussian distribution of $\mathbf{h}_k$ it can be deduced that the elements of $\mathbf{L}$ are independent and l_{mk} is complex Gaussian for $m > k$. On the other hand, the squared column norm

$$\|\mathbf{h}_k\|^2 = \sum_{m=1}^{N_R}|h_{mk}|^2 = l_{kk}^2 + \sum_{m=k+1}^{N_T}|l_{mk}|^2 \tag{10}$$

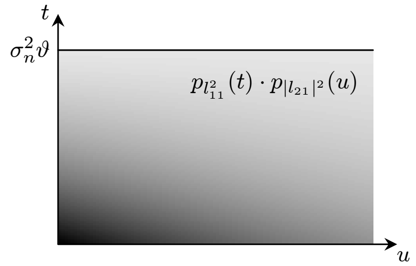

Figure 1: On the calculation of $P_{\mathrm{SNR}_1}(\vartheta \,|\, l_{22}^2 = \xi)$ from the joint pdf of l_{11}^2 and $|l_{21}|^2$ for ZF-SIC.

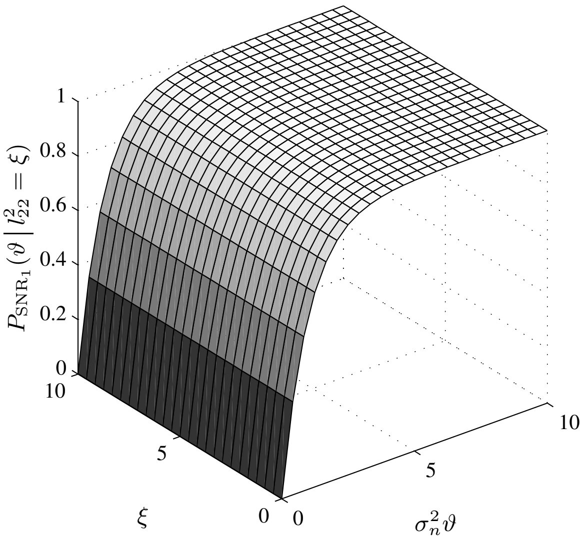

Figure 2: Conditional cdf $P_{\mathrm{SNR}_1}(\vartheta \,|\, l_{22}^2 = \xi)$ for ZF-SIC.

is a sum of N_R exponential random variables; consequently, l_{kk}^2 must be χ^2-distributed with $2(N_R - N_T + k)$ degrees of freedom [11]. This leads to the pdf's

$$p_{l_{kk}^2}(t) = \frac{t^{N_R-N_T+k-1}e^{-t}}{\Gamma(N_R - N_T + k)} \,, \tag{11}$$

$$p_{|l_{mk}|^2}(t) = e^{-t} \,, \quad m > k \tag{12}$$

that are zero for $t < 0$. From (9) and (2) we can now immediately obtain the cdf of the SNR on the k-th layer

$$P_{\mathrm{SNR}_k}(\vartheta) = \Pr\left\{l_{kk}^2 < \sigma_n^2\vartheta\right\} = \tilde{\gamma}(N_R - N_T + k, \sigma_n^2\vartheta) \,. \tag{13}$$

As already mentioned in the introduction, we will focus on the case of two transmit antennas in the following. In order to determine the distribution of SINR_1 for an optimized detection order as well as MMSE interference suppression, it needs to be conditioned on the second layer, as a start. For the unsorted ZF-SIC considered here, this is of course identical to (13) due to the statistical independence of l_{11} and l_{22}. Thus, the conditional cdf shown in Fig. 2 for $N_R = 2$ receive antennas does not depend on ξ at all. Fig. 1 additionally demonstrates how (13) can be calculated by integrating over the joint pdf of l_{11}^2 and $|l_{21}|^2$. These figures serve as a reference for later comparison to illustrate the impact of sorting and MMSE filtering.

5. ZF-SIC WITH OPTIMIZED ORDER

The order of detection is crucial for the performance of SIC. It can be optimized by exchanging elements of the transmit vector $\mathbf{x}$ and the corresponding columns of $\mathbf{H}$. For some permutation matrix $\mathbf{\Pi}$, we define

$$\check{\mathbf{x}} = \mathbf{\Pi}^T \mathbf{x}\,, \quad \check{\mathbf{H}} = \mathbf{H}\mathbf{\Pi}\,, \quad \check{\mathbf{H}} = \check{\mathbf{Q}}\check{\mathbf{L}}\,. \tag{14}$$

It can easily be verified that $\check{\mathbf{H}}\check{\mathbf{x}} = \mathbf{H}\mathbf{x}$, because $\mathbf{\Pi}$ is orthogonal, so the receive vector in (5) is not affected. It was shown in [2] that the minimum SNR among all transmitted streams is maximized by a greedy approach which always chooses the best layer to be detected next. Assuming that the first $k-1$ columns of $\check{\mathbf{H}}$ have already been determined, $\check{\mathbf{h}}_k$ must be selected from the remaining columns of $\mathbf{H}$ such that $\check{l}_{kk}^2$ is as large as possible. As the SNR's after linear ZF filtering with the pseudo-inverse $\check{\mathbf{H}}^+ = \check{\mathbf{L}}^{-1}\check{\mathbf{Q}}^H$ are inversely proportional to the row norms of $\check{\mathbf{G}} = \check{\mathbf{L}}^{-1}$, the conditions

$$\check{g}_{kk}^2 \le \sum_{n=k}^{m} |\check{g}_{mn}|^2 \qquad \forall\, m > k \tag{15}$$

have to be satisfied. For two transmit antennas, (15) becomes

$$\check{\mathbf{G}} = \frac{1}{\check{l}_{11}\check{l}_{22}} \begin{pmatrix} \check{l}_{22} & 0 \\ -\check{l}_{21} & \check{l}_{11} \end{pmatrix} \quad \Rightarrow \quad \check{l}_{22}^2 \le \check{l}_{11}^2 + |\check{l}_{21}|^2\,. \tag{16}$$

Note that this criterion is also employed by the efficient ordering algorithm proposed in [10], where the diagonal elements $\check{l}_{kk}$ are *minimized* in the order they are calculated during the orthogonalization process ($k = N_T, \ldots, 1$) instead of *maximizing* them in the opposite order. However, for $N_T > 2$ this approach is no longer guaranteed to be optimal, though the loss is usually rather small.

5.1 SNR Distribution

From (16) and (10), it can be concluded that for the optimal permutation the squared second diagonal element is

$$\check{l}_{22}^2 = \min\left\{\|\mathbf{h}_1\|^2, \|\mathbf{h}_2\|^2\right\} \tag{17}$$

Hence, we can apply order statistics [11] to obtain the corresponding cdf

$$\begin{aligned} P_{\check{l}_{22}^2}(\xi) =& 1 - \left[\Pr\left\{\|\mathbf{h}_k\|^2 \ge \xi\right\}\right]^2 = 1 - \left[\tilde{\Gamma}(N_R, \xi)\right]^2 \\ =& \tilde{\gamma}(N_R, \xi) \cdot \left[2 - \tilde{\gamma}(N_R, \xi)\right]\,, \end{aligned} \tag{18}$$

and, similar to (13), the distribution of SNR_2 is given by $P_{\mathrm{SNR}_2}(\vartheta) = P_{\check{l}_{22}^2}(\sigma_n^2\vartheta)$. Thus, the outage probability of the second layer is approximately doubled by sorting if $\sigma_n^2\vartheta$ is small, as already noted in [6].

Unfortunately, the diagonal elements of $\check{\mathbf{L}}$ are not independent anymore. However, as both detection orders are equiprobable, the cdf of $\check{l}_{11}^2$ conditioned on $\check{l}_{22}^2 = \xi$ is identical to that of l_{11}^2 under the assumption that the natural ordering $\mathbf{\Pi} = \mathbf{I}_2$ is optimal for $l_{22}^2 = \xi$. With (16) and (9), this leads to the conditional cdf

$$P_{\mathrm{SNR}_1}\left(\vartheta \,\middle|\, \check{l}_{22}^2 = \xi\right) = P_{l_{11}^2}\left(\sigma_n^2\vartheta \,\middle|\, l_{11}^2 + |l_{21}|^2 \ge \xi\right)\,. \tag{19}$$

Exploiting the statistical independence of l_{11} and l_{21}, we start by calculating the joint probability

$$\begin{aligned} &\Pr\left\{l_{11}^2 < \sigma_n^2\vartheta\,,\, l_{11}^2 + |l_{21}|^2 \ge \xi\right\} \\ &= \int_0^{\sigma_n^2\vartheta} \int_{(\xi-t)^+}^{\infty} p_{l_{11}^2}(t) \cdot p_{|l_{21}|^2}(u)\, du\, dt \qquad (20) \\ &= \int_0^{\sigma_n^2\vartheta} \frac{t^{N_R-2}e^{-t}}{\Gamma(N_R-1)} \int_{(\xi-t)^+}^{\infty} e^{-u}\, du\, dt\,, \qquad (21) \end{aligned}$$

where the shorthand notation $(x)^+ = \max\{x, 0\}$ was introduced. The limits of the integrals are illustrated in Fig. 3. Compared to Fig. 1, a significant part of the joint pdf of l_{11}^2 and $|l_{21}|^2$ is disregarded in (20) due to the ordering criterion. For $\sigma_n^2\vartheta > \xi$, we just need to subtract the contribution of the white triangle from (13), while (4) can be applied otherwise to get

$$\begin{aligned} &\Pr\left\{l_{11}^2 < \sigma_n^2\vartheta\,,\, l_{11}^2 + |l_{21}|^2 \ge \xi\right\} \\ &= \begin{cases} (\sigma_n^2\vartheta)^{N_R-1}e^{-\xi}/\Gamma(N_R) & ,\ \sigma_n^2\vartheta \le \xi \\ \tilde{\gamma}(N_R-1, \sigma_n^2\vartheta) - \tilde{\gamma}(N_R, \xi) & ,\ \sigma_n^2\vartheta > \xi\,. \end{cases} \qquad (22) \end{aligned}$$

From (22), we can already deduce the intuitive result that the impact of ordering on the SNR distribution of the first layer is most pronounced if ξ is large; for $\xi = 0$, the constraint (16) is not effective at all. On the other hand, taking

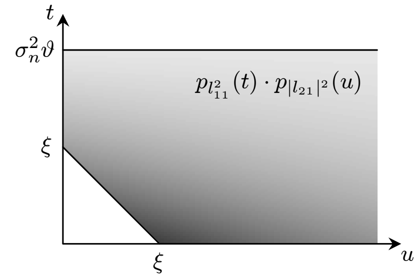

Figure 3: On the calculation of $P_{\mathrm{SNR}_1}(\vartheta \,|\, \check{l}_{22}^2 = \xi)$ from the joint pdf of l_{11}^2 and $|l_{21}|^2$ for ordered ZF-SIC.

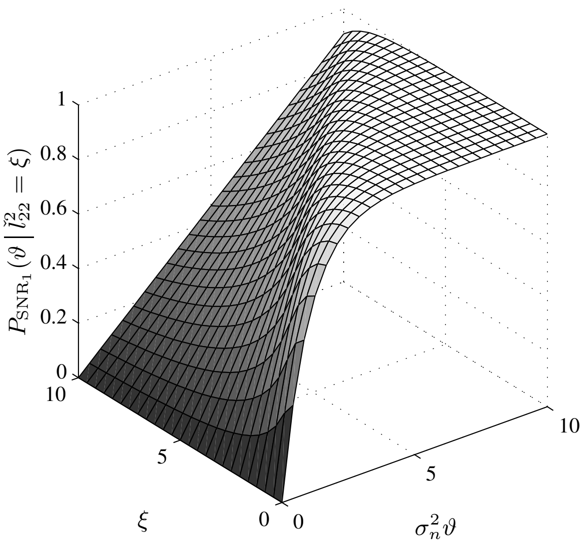

Figure 4: Conditional cdf $P_{\mathrm{SNR}_1}(\vartheta \,|\, \check{l}_{22}^2 = \xi)$ for ordered ZF-SIC.

the limit $\sigma_n^2\vartheta \to \infty$ yields

$$\Pr\left\{l_{11}^2 + |l_{21}|^2 \geq \xi\right\} = 1 - \tilde{\gamma}(N_R, \xi) = \tilde{\Gamma}(N_R, \xi)\ , \qquad (23)$$

which is the complementary cdf of $\|\mathbf{h}_k\|^2$, so the conditional cdf in (19) is given by

$$P_{\mathrm{SNR}_1}(\vartheta \,|\, \tilde{l}_{22}^2 = \xi) = \frac{\Pr\left\{l_{11}^2 < \sigma_n^2\vartheta\, ,\, l_{11}^2 + |l_{21}|^2 \geq \xi\right\}}{\Pr\left\{l_{11}^2 + |l_{21}|^2 \geq \xi\right\}}$$
$$= \begin{cases} (\sigma_n^2\vartheta)^{N_R-1}e^{-\xi}/\Gamma(N_R,\xi) & ,\ \sigma_n^2\vartheta \leq \xi \\ 1 - \tilde{\Gamma}(N_R-1, \sigma_n^2\vartheta)/\tilde{\Gamma}(N_R,\xi) & ,\ \sigma_n^2\vartheta > \xi\ . \end{cases} \qquad (24)$$

Fig. 4 again shows an example for $N_R = 2$. Comparing this to Fig. 2, we find that optimal ordering reduces the outage probability of the first layer for any given $\xi > 0$, and especially for large values, as expected. Hence, the unconditional cdf of SNR_1, which can be computed by averaging (24) over $\tilde{l}_{22}^2$, will also be decreased. The required pdf of $\tilde{l}_{22}^2$ is obtained by taking the derivative of (18)

$$p_{\tilde{l}_{22}^2}(\xi) = \frac{2\xi^{N_R-1}e^{-\xi}}{\Gamma(N_R)}\tilde{\Gamma}(N_R, \xi)\ . \qquad (25)$$

With this, we finally arrive at

$$P_{\mathrm{SNR}_1}(\vartheta) = \int_0^\infty P_{\mathrm{SNR}_1}(\vartheta \,|\, \tilde{l}_{22}^2 = \xi) \cdot p_{\tilde{l}_{22}^2}(\xi)\, d\xi \qquad (26)$$
$$= \frac{(\sigma_n^2\vartheta/2)^{N_R-1}\tilde{\Gamma}(N_R, 2\sigma_n^2\vartheta)}{\Gamma(N_R)} + 1 - \left[\tilde{\Gamma}(N_R, \sigma_n^2\vartheta)\right]^2$$
$$- 2\tilde{\Gamma}(N_R-1, \sigma_n^2\vartheta) \cdot \tilde{\gamma}(N_R, \sigma_n^2\vartheta)\ . \qquad (27)$$

The first term belonging to the case $\sigma_n^2\vartheta \leq \xi$ in (24) results from (1) after the substitution $\xi' = 2\xi$, and the other ones immediately follow from (18) and (2). Note that (27) can also be rewritten in terms of exponential functions and polynomials using the relations in (1) and (2).

6. MMSE-SIC WITHOUT ORDERING

Following the approach of [12], we first define the QL decomposition of the extended channel matrix

$$\underline{\mathbf{H}} = \begin{pmatrix} \mathbf{H} \\ \sigma_n \mathbf{I}_{N_T} \end{pmatrix} = \begin{pmatrix} \mathbf{Q}_1 \\ \mathbf{Q}_2 \end{pmatrix} \underline{\mathbf{L}}\ . \qquad (28)$$

Then, using $\mathbf{H} = \mathbf{Q}_1\underline{\mathbf{L}}$ it can easily be verified that the linear MMSE filter for the system model (5) is given by

$$(\mathbf{H}^H\mathbf{H} + \sigma_n^2\mathbf{I}_{N_T})^{-1}\mathbf{H}^H = (\underline{\mathbf{H}}^H\underline{\mathbf{H}})^{-1}\mathbf{H}^H = \underline{\mathbf{L}}^{-1}\mathbf{Q}_1^H\ . \qquad (29)$$

Hence, MMSE-SIC is identical to the ZF-SIC described in Section 4 with $\mathbf{Q}$ and $\mathbf{L}$ being replaced by $\mathbf{Q}_1$ and $\underline{\mathbf{L}}$, respectively, and the filter output signal becomes

$$\underline{\mathbf{z}} = \mathbf{Q}_1^H\mathbf{y} = \underline{\mathbf{L}}\mathbf{x} - \sigma_n\mathbf{Q}_2^H\mathbf{x} + \mathbf{Q}_1^H\tilde{\mathbf{n}}\ ; \qquad (30)$$

the second term in (30) represents a bias and remaining interference. Using the relations $\mathbf{Q}_1^H\mathbf{Q}_1 + \mathbf{Q}_2^H\mathbf{Q}_2 = \mathbf{I}_{N_T}$ and $\mathbf{Q}_2 = \sigma_n\underline{\mathbf{L}}^{-1}$, which follow from the properties of the QL decomposition in (28), we find that the SINR of layer k assuming no errors in previous detection steps is given by

$$\mathrm{SINR}_k = \frac{\left(\underline{l}_{kk} - \sigma_n^2/\underline{l}_{kk}\right)^2}{\sigma_n^2 - \sigma_n^4/\underline{l}_{kk}^2} = \frac{\underline{l}_{kk}^2}{\sigma_n^2} - 1\ . \qquad (31)$$

This of course equals the SNR for the second layer, as the interference has already been subtracted completely. Thus, we can use the results derived for ZF-SIC and concentrate on the first layer. Observing that $\|\underline{\mathbf{h}}_k\|^2 = \|\mathbf{h}_k\|^2 + \sigma_n^2$ and $|\underline{\mathbf{h}}_2^H\underline{\mathbf{h}}_1|^2 = l_{22}^2|l_{21}|^2$, we obtain

$$\underline{l}_{11}^2 = \|\underline{\mathbf{h}}_1\|^2 - |\underline{\mathbf{h}}_2^H\underline{\mathbf{h}}_1|^2/\|\underline{\mathbf{h}}_2\|^2 \qquad (32)$$
$$= l_{11}^2 + \sigma_n^2 + \frac{\sigma_n^2|l_{21}|^2}{l_{22}^2 + \sigma_n^2}\ , \qquad (33)$$

which can be plugged into (31) to get

$$\mathrm{SINR}_1 = \frac{l_{11}^2}{\sigma_n^2} + \frac{|l_{21}|^2}{l_{22}^2 + \sigma_n^2}\ . \qquad (34)$$

Note that (34) corresponds to the SNR_1 of ZF-SIC in (9) for $l_{22}^2 \to \infty$, while it has the same distribution as SNR_2 for $l_{22}^2 = 0$. Thus, unlike the linear ZF filter, the MMSE filter benefits from small SNR's on the second layer, because less interference needs to be suppressed.

6.1 SINR Distribution

From (34) it follows that the SINR distribution of the first layer conditioned on $l_{22}^2 = \xi$ can be calculated by integrating the joint pdf of l_{11}^2 and $|l_{21}|^2$ over the region sketched in

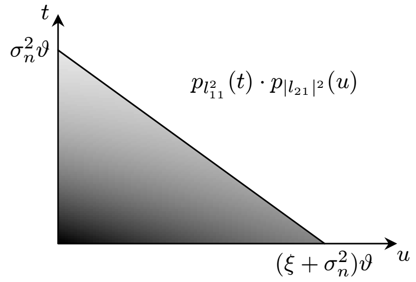

Figure 5: On the calculation of $P_{\mathrm{SINR}_1}(\vartheta \,|\, l_{22}^2 = \xi)$ from the joint pdf of l_{11}^2 and $|l_{21}|^2$ for MMSE-SIC.

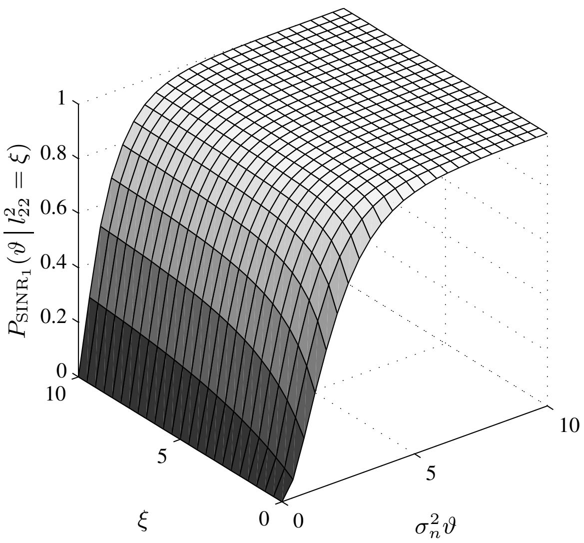

Figure 6: Conditional cdf $P_{\mathrm{SINR}_1}(\vartheta \,|\, l_{22}^2 = \xi)$ for MMSE-SIC.

Fig. 5. With (2) and (3) we get

$$P_{\mathrm{SINR}_1}(\vartheta \,|\, l_{22}^2 = \xi) = \Pr\left\{ \frac{l_{11}^2}{\sigma_n^2} + \frac{|l_{21}|^2}{\xi + \sigma_n^2} < \vartheta \right\}$$

$$= \int_0^{\sigma_n^2\vartheta} \frac{t^{N_R-2} e^{-t}}{\Gamma(N_R-1)} \int_0^{[\xi+\sigma_n^2]\vartheta - \frac{\xi+\sigma_n^2}{\sigma_n^2} t} e^{-u}\, du\, dt \qquad (35)$$

$$= \tilde{\gamma}(N_R-1, \sigma_n^2\vartheta) - \frac{e^{-(\xi+\sigma_n^2)\vartheta}\, \tilde{\gamma}(N_R-1, -\vartheta\xi)}{(-\xi/\sigma_n^2)^{N_R-1}}\,. \qquad (36)$$

In line with the above observations, the first term is the cdf of SNR_1 for ZF-SIC, while the other one vanishes for $\xi \to \infty$, and becomes $e^{-\sigma_n^2\vartheta}(\sigma_n^2\vartheta)^{N_R-1}/\Gamma(N_R)$ for $\xi \to 0$, so that the cdf converges to $\tilde{\gamma}(N_R, \sigma_n^2\vartheta)$. An example for $N_R = 2$ and $\sigma_n^2 = 1$ is shown in Fig. 6. Here, the conditional outage probability decreases for small values of ξ. This is just opposite to the case of ordered ZF-SIC in Fig. 4, where a large ξ improves the performance of the first layer.

Noting that (4) tends to $-c^n/([c-b]^n b)$ for $b < c < 0$ and $a \to \infty$, the unconditional cdf

$$P_{\mathrm{SINR}_1}(\vartheta) = \int_0^\infty P_{\mathrm{SINR}_1}(\vartheta \,|\, l_{22}^2 = \xi) \cdot p_{l_{22}^2}(\xi)\, d\xi$$

$$= \tilde{\gamma}(N_R-1, \sigma_n^2\vartheta) - \frac{(\sigma_n^2\vartheta)^{N_R-1} e^{-\sigma_n^2\vartheta}}{\Gamma(N_R)\cdot[\vartheta+1]} \qquad (37)$$

can also easily be determined. In contrast to ZF interference suppression it does not only depend on the product $\sigma_n^2\vartheta$, but also on ϑ itself.

7. MMSE-SIC WITH OPTIMIZED ORDER

We now finally turn to the case of ordered MMSE-SIC. Similar to Section 5, the permutation must be chosen such that the diagonal element $\breve{l}_{22}^2$ is as small as possible in order to maximize SINR_1. However, this now additionally means that less interference needs to be suppressed by the linear MMSE filter in the first step. Hence, it may already be conjectured that the impact of sorting is much more pronounced for MMSE-SIC. The derivation of the SINR distribution is similar to those for ordered ZF-SIC, so we will subsequently focus on the main results and omit intermediate steps.

7.1 SINR Distribution

Combining Fig. 3 with Fig. 5, we find that the joint pdf of l_{11}^2 and $|l_{21}|^2$ must be integrated over the region depicted in Fig. 7 in order to obtain the joint probability

$$\Pr\left\{ \frac{l_{11}^2}{\sigma_n^2} + \frac{|l_{21}|^2}{\xi+\sigma_n^2} < \vartheta\,,\, l_{11}^2 + |l_{21}|^2 \geq \xi \right\} \qquad (38)$$

$$= \begin{cases} 0 & ,\ \xi \geq [\xi+\sigma_n^2]\vartheta \\ \frac{[\xi-(\xi+\sigma_n^2)\vartheta]^{N_R-1} e^{-\xi}}{\Gamma(N_R)\cdot(-\xi/\sigma_n^2)^{N_R-1}} - \frac{e^{-(\xi+\sigma_n^2)\vartheta}\tilde{\gamma}(N_R-1, \xi-[\xi+\sigma_n^2]\vartheta)}{(-\xi/\sigma_n^2)^{N_R-1}} & ,\ \sigma_n^2\vartheta \leq \xi < [\xi+\sigma_n^2]\vartheta \\ \tilde{\gamma}(N_R-1, \sigma_n^2\vartheta) - \tilde{\gamma}(N_R, \xi) - \frac{e^{-(\xi+\sigma_n^2)\vartheta}\tilde{\gamma}(N_R-1, -\vartheta\xi)}{(-\xi/\sigma_n^2)^{N_R-1}} & ,\ \sigma_n^2\vartheta > \xi\,. \end{cases}$$

In the second case, the two boundaries $(\xi+\sigma_n^2)(\vartheta - t/\sigma_n^2)$ and $\xi - t$ intersect, while the third case directly follows from (22) and (36). For $\sigma_n^2\vartheta \to \infty$ we get (23) again. Thus, dividing (38) by $\tilde{\Gamma}(N_R, \xi)$ yields the cdf of SINR_1 with optimal sorting conditioned on $\breve{l}_{22}^2 = \xi$

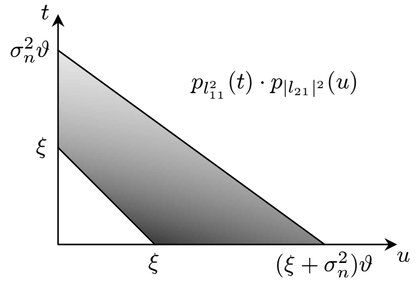

Figure 7: On the calculation of $P_{\mathrm{SINR}_1}(\vartheta \,|\, \breve{l}_{22}^2 = \xi)$ from the joint pdf of l_{11}^2 and $|l_{21}|^2$ for ordered MMSE-SIC.

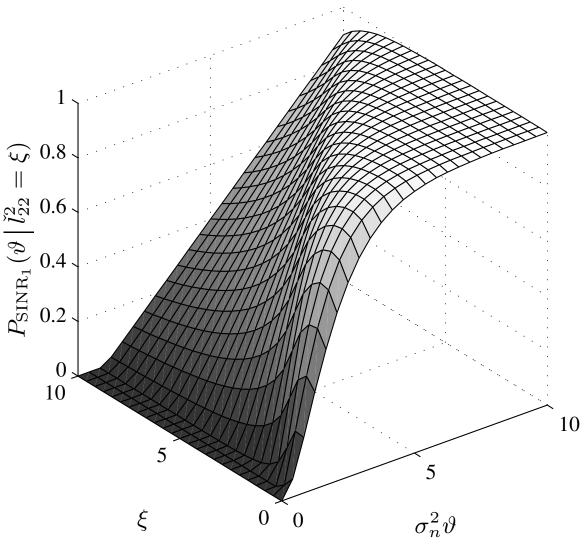

Figure 8: Conditional cdf $P_{\mathrm{SINR}_1}(\vartheta \,|\, \breve{l}_{22}^2 = \xi)$ for ordered MMSE-SIC.

$$P_{\mathrm{SINR}_1}(\vartheta \,|\, \breve{l}_{22}^2 = \xi) \qquad (39)$$

$$= \begin{cases} 0 & ,\ \xi \geq [\xi+\sigma_n^2]\vartheta \\ \frac{[\xi-(\xi+\sigma_n^2)\vartheta]^{N_R-1} e^{-\xi}}{\Gamma(N_R,\xi)\cdot(-\xi/\sigma_n^2)^{N_R-1}} - \frac{e^{-(\xi+\sigma_n^2)\vartheta}\tilde{\gamma}(N_R-1, \xi-[\xi+\sigma_n^2]\vartheta)}{\tilde{\Gamma}(N_R,\xi)\cdot(-\xi/\sigma_n^2)^{N_R-1}} & ,\ \sigma_n^2\vartheta \leq \xi < [\xi+\sigma_n^2]\vartheta \\ 1 - \tilde{\Gamma}(N_R-1, \sigma_n^2\vartheta)/\tilde{\Gamma}(N_R, \xi) - \frac{e^{-(\xi+\sigma_n^2)\vartheta}\tilde{\gamma}(N_R-1, -\vartheta\xi)}{\tilde{\Gamma}(N_R,\xi)\cdot(-\xi/\sigma_n^2)^{N_R-1}} & ,\ \sigma_n^2\vartheta > \xi\,. \end{cases}$$

In order to avoid numerical problems, the incomplete gamma functions with negative second argument in (39) should be replaced by the polynomial representation in (1), and the exponential relation $e^a \cdot e^b = e^{a+b}$ should be applied.

From Fig. 8 it can be observed that the outage probability is significantly reduced for all values of ξ. For small ξ this is mainly a consequence of MMSE filtering, while for large ξ sorting plays a major role. The unconditional cdf is again calculated by taking the expectation of (39) over $\breve{l}_{22}^2$. With adequate substitutions we can use (4) to obtain after some simplifications

$$
\begin{aligned}
P_{\mathrm{SINR}_1}(\vartheta) = & 1 - \left[\tilde{\Gamma}(N_R, \sigma_n^2 \vartheta)\right]^2 \\
& - 2\tilde{\Gamma}(N_R - 1, \sigma_n^2 \vartheta) \cdot \tilde{\gamma}(N_R, \sigma_n^2 \vartheta) \\
& + \frac{(-\sigma_n^2)^{N_R-1}}{\Gamma(N_R)} \left[\frac{(-\sigma_n^2 \vartheta^2)^{N_R-1}}{\Gamma(N_R)} e^{-2\sigma_n^2 \vartheta} \right. \\
& - \frac{2(-\vartheta)^{N_R-1}}{\vartheta + 1} e^{-\sigma_n^2 \vartheta} \tilde{\gamma}(N_R - 1, \sigma_n^2 \vartheta) \\
& \left. + \frac{(1-\vartheta)^{N_R} e^{\frac{2\sigma_n^2 \vartheta}{\vartheta - 1}}}{2^{N_R-1}(\vartheta + 1)} \Upsilon\left(N_R - 1, \frac{2\sigma_n^2 \vartheta^2}{\vartheta - 1}\right) \right]
\end{aligned} \tag{40}
$$

$$
\text{with } \Upsilon(n, x) = \begin{cases} \tilde{\gamma}(n, x) & , \; x \leq 0 \\ -\tilde{\Gamma}(n, x) & , \; x > 0 \; . \end{cases} \tag{41}
$$

The two different cases must be distinguished, because the first condition in (39) is never fulfilled for $\vartheta \geq 1$, which affects the limits of the integrals.

8. NUMERICAL RESULTS

Fig. 9 depicts the layer-wise SINR distributions for a multiple antenna system with two transmit and receive antennas. The thin lines represent the second layer with no, optimal, or inverted sorting, i.e. $\tilde{l}_{22}^2 = \max\{\|\mathbf{h}_1\|^2, \|\mathbf{h}_2\|^2\}$. As already noted in Section 5, optimal sorting approximately doubles the outage probability in this detection step. In contrast, the curve of the first layer is shifted to the right by 3 dB for ZF-SIC. The three different curves for MMSE-SIC belong to increasing noise variances (from left to right). For strong noise, the interference can be neglected, and the SINR distribution is close to that of the second layer with the inverse ordering applied. On the other hand, for small values of σ_n^2, MMSE-SIC performs similar to ZF-SIC over a wide range, but eventually decreases for sufficiently small ϑ. With optimal sorting, the outage probability rapidly converges to the interference-free case for $\vartheta < 1$, while a constant gap remains without optimized detection order.

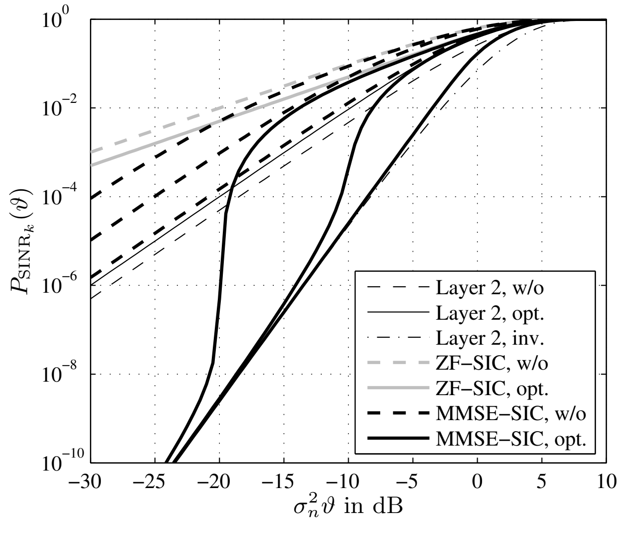

Figure 9: SINR distributions for $N_T = N_R = 2$ and $\sigma_n^2 \in \{0.01, 0.1, 1\}$ (required only for MMSE-SIC).

9. CONCLUSION

We have presented a new unified approach to the SINR analysis of V-BLAST with (ordered) ZF- or MMSE-SIC detection. Based on geometrical considerations, the SINR distribution of the first layer was calculated for different receiver architectures by first conditioning on, and then averaging over the effective channel gain of the second layer. The effects of an optimized detection order and MMSE interference suppression were investigated separately and visualized by means of the conditional cdf of SINR_1. Furthermore, it was shown analytically that the optimal ordering is even more important in combination with MMSE filtering.

10. REFERENCES

[1] E. Telatar, "Capacity of Multi-antenna Gaussian Channels," *European Transactions on Telecommunications*, vol. 10, no. 6, pp. 585–595, November-December 2000.

[2] P. W. Wolniansky, G. J. Foschini, G. D. Golden, and R. A. Valenzuela, "V-BLAST: An Architecture for Realizing Very High Data Rates Over the Rich-Scattering Wireless Channel," in *Proc. ISSSE*, Pisa, Italy, September 1998.

[3] M. Kießling, "Statistical Analysis and Transmit Prefiltering for MIMO Wireless Systems in Correlated Fading Environments," Ph.D. dissertation, Institut für Nachrichtenübertragung, Universität Stuttgart, 2004.

[4] G. J. Foschini, G. D. Golden, A. Valenzela, and P. W. Wolniansky, "Simplified Processing for High Spectral Efficiency Wireless Communications Emplying Multi-Element Arrays," *IEEE Journal on Selected Areas in Commununications*, vol. 17, no. 11, pp. 1841–1852, November 1999.

[5] A. Kannan, B. Varadarajan, and J. Barry, "Joint Optimization of Rate Allocation and BLAST Ordering to Minimize Outage Probability," in *Proc. IEEE Wireless Communications and Networking Conference*, New Orleans, USA, March 2005.

[6] S. Loyka, "V-BLAST Outage Probability: Analytical Analysis," in *Proc. IEEE Vehicular Technology Conference (VTC)*, Vancouver, Canada, September 2002.

[7] S. Loyka and F. Gagnon, "Analytical Framework for Outage and BER Analysis of the V-BLAST Algorithm," in *Proc. International Zurich Seminar on Communications*, Zurich, Switzerland, February 2004.

[8] R. Xu and F. Lau, "Analytical Approach of V-BLAST Performance with Two Transmit Antennas," in *Proc. IEEE Wireless Communications and Networking Conference*, New Orleans, USA, March 2005.

[9] I. Gradshteyn and I. Ryzhik, *Table of Integrals, Series and Products*, 6th ed. San Diego, CA: Academic Press, 2000.

[10] D. Wübben, R. Böhnke, J. Rinas, V. Kühn, and K. D. Kammeyer, "Efficient Algorithm for Decoding Layered Space-Time Codes," *IEE Electronics Letters*, vol. 37, no. 22, pp. 1348–1350, October 2001.

[11] A. Papoulis, *Probability, Random Variables, and Stochastic Processes*, 3rd ed. New York: McGraw-Hill, 1991.

[12] R. Böhnke, D. Wübben, V. Kühn, and K. D. Kammeyer, "Reduced Complexity MMSE Detection for BLAST Architectures," in *Proc. IEEE Global Communications Conference (Globecom'03)*, San Francisco, California, USA, December 2003.